Densenet Model for Binary Glaucoma Classification Performance Assessment with Texture Feature

Wildan Jameel Hadi* ⁱᴰ ✉, **Amal Sufiuh Ajrash** ⁱᴰ ✉, **Sahar Muneam Salman** ⁱᴰ ✉, **Mays jalal jasim** ⁱᴰ ✉, **Mina Taha Ibrahim** ⁱᴰ ✉

Department Computer Science, College of Science for Women, University of Baghdad, Baghdad, Iraq.
*Corresponding Author.

Abstract

The retina is an important portion of the eye because images of it are used by doctors to diagnose numerous eye diseases such as glaucoma, diabetic retinopathy, and cataracts. Indeed, segmented retinal imaging is a powerful tool for detecting unusual growths in the eye area as well as determining the size and structure of the optic disc. The combination of digital image processing and deep learning techniques enables the development of automated approaches for detecting glaucoma. Within this framework, the objective of this study is to achieve prompt detection of glaucoma by utilizing a DenseNet-121 Network in conjunction with texture qualities derived from local binary patterns (LBP). The proposed method can be categorized into four steps: (i) obtaining images from the OIH public database; (ii) preprocessing the images by extracting texture attributes using LBP; (iii) classifying glaucoma images and normal images using a DenseNet-121 network; and (iv) validating the proposal based on performance metrics. Based on the results of the proposed strategy, the accuracy remains approximately 96%.

Keywords: Binary Classification, Dense Net, Eye Diseases, LBP, Texture.

Introduction

A very thin layer that lines the interior of the back of the eye is called the retina. It does this by transforming the light that enters the eye into nerve signals, which are subsequently transmitted to the optical cortex of the brain, where they are processed for object recognition[1]. Eye illnesses that go undiagnosed can cause permanent damage to the retina, which can lead to a loss of eyesight. As a result, early diagnosis is necessary in order to receive the proper treatment [2]. Glaucoma is an eye disease that affects humans and is caused by damage to the optic nerve, which is located at the rear of the eye. This form of disease does not manifest symptoms until it has reached an advanced stage. Because of this, glaucoma is referred to as the silent thief of

sight, as a person cannot detect the disease unless he endures a thorough examination of the dilated eye. In fact, there is no cure for this disease, but it can be prevented through early detection[3]. Typically, an eye examination involves taking an image of the retina, which must be manually examined by an expert eye doctor to determine whether or not glaucoma symptoms are present. The examination of retinal images is typically performed by highly trained clinicians to assure the accuracy of the diagnosis; this takes time [4]. This periodic examination typically requires ophthalmologists to exert considerable effort to examine the images of all patients, some of whom may not be infected. Therefore, relying on an

automated examination system can be advantageous for patients as well as doctors.

The retina images are utilized to evaluate blood vessels, vascular structures, hemorrhage, neovascularization, and all secretions to determine whether the fundus images are abnormal. In reality, the damage to the optic nerve in the patient's retina is witnessed when the eye is affected by glaucoma disorders by increasing the size of the cup of the optic disc and modifying its features about the optical disk[5]. Fig. 1 shows a glaucoma-affected eye retina compared to a normal eye. Despite the implementation of many techniques, accurately identifying optic nerve damage in retinal fundus images remains a significant difficulty. Challenges include the presence of brighter patches in the central part of the retina and darker regions in the periphery. Accordingly, certain studies have suggested utilizing a texture-based method to maintain the integrity of the fundus structure. Local binary patterns (LBP) are a frequently used type of texture features.

(a)   (b)
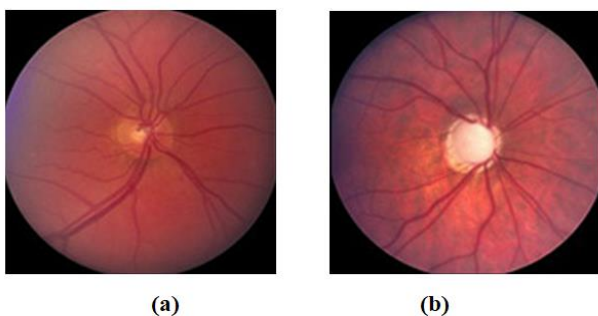
Figure 1. Retina examples Normal (a) and Glaucoma (b).

In fact, there are exceptional efforts by the industrial and academic communities to rely on Convolutional neural network (CNN) models to design reliable

techniques for analyzing images [6-8]. This contribution came about because CNN models have proven effective in classification problems. Therefore, using such models supports doctors' decisions by reducing the burden on them and reducing the time required to detect glaucoma. In general, most eye diseases in their early stages are similar in clinical signs, and here comes the role of CNN in extracting the subtle and hidden features that lie in the input fundus images and using them as an indicator for detecting the disease[9]. The following are some of the significant contributions that this work makes:

- The majority of earlier efforts only trained small datasets. For example, the latest work described by [10] constructs the model utilizing datasets including 400 RGB images. Instead, in order to ensure that the model can detect different types of glaucoma images, we train the deep network on a large-scale dataset termed OIH. It is worth noting that the suggested deep learning pipeline can achieve 96% accuracy, but classical SVM 11 can only get 83,33% accuracy with comparable conditions.

- A thorough assessment of glaucoma detection via the LBP texture feature is presented. To ensure utmost precision, we implement the most recent deep learning methodology, specifically DenseNet-121. It is imperative to acknowledge that the recent study put forth by [10] utilizes an older architectural model known as VGG16 for the purpose of DR image detection. Regrettably, despite employing the exact hyperparameter configuration, the VGG16 achieves a mere 76.21% accuracy on this enormous dataset.

Related work

Methods for detecting glaucoma diseases in the retina images are varied, but in general, the research literature classifies them into three categories: general, structural, and hybrid [3].

As for generic methods, they typically involve analyzing the properties of the optical disk area. This is accomplished by extracting and analyzing the texture and statistical properties calculated from the image's spatial or wavelet domains. The authors of [11] created a method to distinguish normal and abnormal glaucoma eye images using automatic ocular

ultrasound analysis. The most difficult issues in automatic glaucoma recognition are feature extraction from retinal pictures and feature categorization based on the recovered features. Image-derived features are classed as structural or textural. To extract features, a discrete wavelet transforms (DWT) integrating daubechies, symlets, and biorthogonal wavelets is used. A Probabilistic Neural Network identifies ocular images as normal or abnormal. Finally, this classifier is capable of distinguishing between normal and glaucomatous

images. By automatically constructing ROIs, [12] suggested two inventive algorithms for segmenting the optic disc and optic cup borders. The first method segments optic disk using the inverse polar transform and ROI's sixth-level Daubechies stationary wavelet transform horizontal coefficients. Using the maximum vessel pixel sum to acquire the entire optic cup region, the second method extends partial cup edges to the nasal side of the cup border. Singh et al. [13] calculated the mean and energy of the optic disc region's first wavelet level detail subbands to distinguish between normal and glaucomatous images. A dataset of 63 images, of which 70% were used for training and the remainder for testing, yielded an accuracy of 94.7% for both SVM and KNN classifiers. Singh et al. discovered that the wavelet features of the optic disc were more clinically significant than the image features of the retina.

The structural methods for discovering glaucoma are mainly dependent on the expense of structural measurements that are brought up by the segmentation of both the cup and the optical disk in order to determine whether the disease is present or not domains of the image [3]. Common glaucoma detection methods are based on the segmentation of the optic cup and optic disk and the calculation of the cup-to-disc ratio [14, 15]. One example is relying on the vertical cup-to-disc ratio to detect glaucoma, by using three segmentation algorithms that segment the optic disc area. the segmentation algorithms used by the researcher include clustering-based techniques, Thresholding-based methods, and region-based techniques [16]. Another example of glaucoma detection is based on texture and structural features.

The researchers relied on extracting several features to help detect glaucoma, including texture features obtained from a histogram of gradient (HOG), entropy of images, Grey-Level Co-occurrence Matrix (GLCM) and structural features such as rim-to-disc ratio (RDR), cup to disk ratio (CDR)[17]. The structural approaches for glaucoma detection significantly rely on the correct segmentation of the cup and optical disk from inserted retina images. Moreover, we guarantee that the proposed solutions will be effective if segmentation of both the optical disk and the cup is implemented correctly. In other instances, however, it is impossible to distinguish between the cup and the disk, making segmentation difficult. At the present time, the segmentation algorithms cross and take a long time to get good results, which makes them inappropriate in automatic retinal check -in systems [18- 20].

For hybrid methods to detect glaucoma, statistical and textual features of general methods must be combined with structural methods that rely primarily on the segmentation of the optical disk and the cup. Since structural methods serve as the foundation for hybrid approaches, the latter are susceptible to the limitations of structural glaucoma detection methods [3]. In[21] glaucomatous retinal images were classified using a combination of intensity and textural features along with several structural features calculated from the segmented optic disc and cup. Using a tenfold cross-validated SVM classifier, the proposed algorithm achieved accuracies of 83% for structural features and 94% for textural features. These findings demonstrate that textural characteristics are superior to structural ones for glaucoma classification.

Materials and Methods

This section lists methods and materials for identifying glaucoma by first generating texture images from eye retina fundus images using the LBP. The generated texture images are then fed into a binary classification system that employs the deep-learning algorithm DenseNet-121 to classify them as normal or abnormal (glaucoma), as illustrated in Fig. 2.
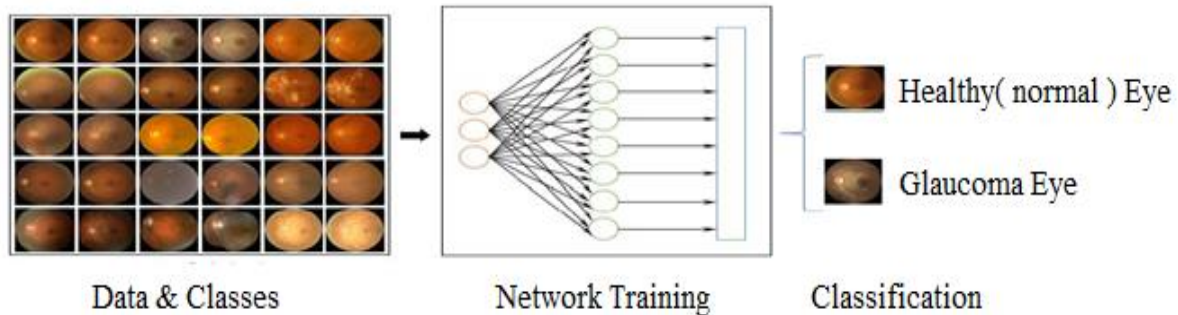
Figure 2. Proposed method steps.

Results and Discussion

Dataset

CFB images of the eye disease dataset constitutes the database used to evaluate the performance and generalizability of the proposed method. This image dataset was compiled from numerous sources, including the Indian Diabetic Retinopathy Image Dataset (IDRiD), Oculur Recognition, and High-Resolution Fundus (HRF). The name of this dataset is the OIH dataset [22]. About 4,000 images covering three types of eye illnesses and one type of normal eye are included in this database. The image sizes utilized in the database range from 640*480 to 1050*1050 and 2416*1736. The images in this study were resized to 224*224 before the texture maps were retrieved. The diagnosis of glaucoma for each image entered was documented based on medical professionals' diagnoses. All input retinal fundus color images are transformed to grayscale as a pre-processing stage before texture maps are produced using LBP. The cataract and diabetic retinopathy classes have 1038 and 1098 images; the dataset is almost balanced. Normal has 1074 images and glaucoma 1007 images. Sample CFP images for the ophthalmic dataset of class Normal are shown in Fig. 3.
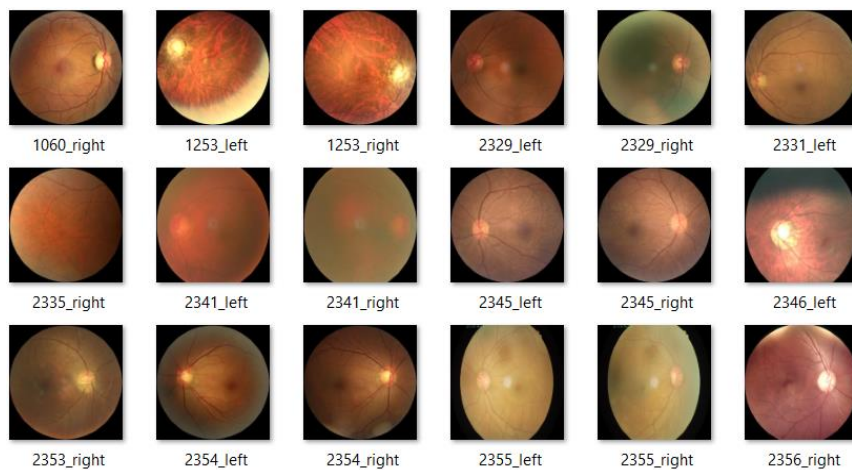
Figure 3. Examples of CFP images.

Texture Extraction

In this section, we describe how LBP is used to generate texture images from the retinal fundus images of the eye. In computer applications such as face detection and face recognition, LBP is an effective textural operator [23]. LBP descriptors are able to effectively capture the local spatial patterns and grayscale contrast in an image. A threshold value distinguishes the center-point pixel from its neighbor pixel in LBP, where the neighborhood is a 3x3 window. The window center's gray value is used as a threshold to compare to the eight neighboring pixels. If the surrounding pixel's gray value is larger than the center pixel's, the pixel is marked 1; otherwise, 0. The window LBP shows local texture information. By finding the local image edge with the LBP operator, we may detect distinct entities in images. This feature descriptor is computed for every pixel in the input image as given below:

$$LBP(P,R) = \sum_{p=0}^{p-1} f(g_p - g_c) 2^p \qquad 1$$

Where g_p and g_c represent the respective intensities of the current and neighboring pixels. P is a number of pixels selected within a radius R [24]. The reason for employing LBP is that when glaucoma affects the eye, the dimensions and properties of the optical disk and the visual nerve head change substantially when compared to a healthy eye, allowing edges to be easily observed in texture images. Fig. 4 shows the variations in the LBP texture generations for the images used in Fig. 1.
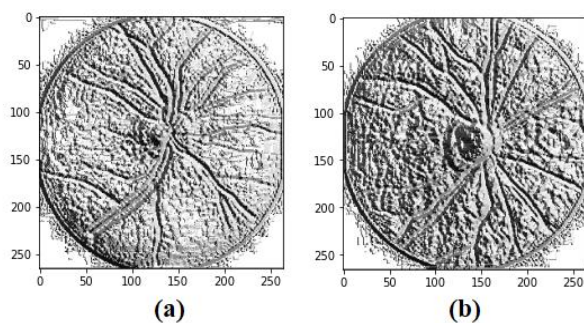
Figure 4. Extraction LBP texture images.

Augmenting and Normalizing Data

It is the step that comes after extracting texture data from the retinal fundus images. In fact, extracting new data from existing data using image processing and simple manipulations is referred to as data augmentation or transformation. The model will become more generalized with the help of augmentation, which will also prevent it from overfitting to the training outcomes. This is accomplished by adding new data without having to spend a lot of time doing it manually. There are ready-made tools in Python that perform this process very quickly. The Image Data Generator class is being used to augment the textured retinal fundus dataset. Augmentation utilizes the zoom, rotation, horizontal_flip, width_shift, height_shift, and rescale methods. Scaling is required for image normalization. The range of the zoom function is set to 0.2, and the shift for both width and height is set to 0.1.

Training and Validation

The textured retinal eye dataset is divided into an 80:20 ratio so that the model can be trained and validated using a variety of different datasets. This automatically labels the images that are contained within each folder whose name is derived from the class name. The tagged images and tracks of the train are loaded by DataLoader, which also loads the train's data (image) and label (class name). This organizes our dataset into two classes: the first class is labeled as having retinal eyes that are normal and healthy, while the second class is labeled as having retinal eyes that have glaucoma. After the classes have been prepared, the data can be put into CUDA (on the GPU) or the CPU before proceeding to the model.

Binary Classification

We need a deep learning model to complete the process of binary classification between retinal images with glaucoma and healthy retinal images. The DenseNet-121 model was chosen because its architecture sets it apart from other models and improves generalization performance. DenseNets do not need to learn superfluous features, so they require fewer parameters than other CNN models. The layers of DenseNets are thin and they generate a negligible number of new feature maps [25]. The reusing of features is the core philosophy behind DenseNet, which ultimately leads to versions that are very little in size. As a consequence of this, it requires a smaller number of parameters than other CNNs do because there is no replication of feature maps. When CNN investigates further, they run into problems. The reason for this is due to the fact that the mapping of data from the inner layer to the outer layer (as well as the gradient in the other direction) is so long that it is possible for it to disappear before arriving any further side. This connectivity is made significantly simpler by DenseNet, which does nothing more than connect every layer directly with every other layer. DenseNets make efficient use of the available capacity of the network by reusing its characteristics [26]. According to the information provided in, a DenseNet is a type of convolutional neural network, and a typical DenseNet architecture makes use of dense blocks to link all layers (with corresponding feature-map sizes) directly to each other, which results in dense connections between layers.

The name "DenseNet" signifies that the network's accuracy will improve as the number of connections increases. DenseNet is built in layers, and each layer transmits its own feature maps to the layers that come after it while also receiving additional input from the layers that came before it. The idea of concatenation, which describes the process by which each layer is given the aggregate knowledge of the layers that lie above it, is utilized here. Integrating many classifiers into an ideal and deep convolutional neural network and interconnecting them with dense connections is

one way to achieve effective image categorization [27]. Convolutional neural networks that have short connections between layers and those that are close to the output have been proven to be capable of being substantially deeper and will be a lot more accurate when trained [28]. DenseNet delivers significant gains over the state-of-the-art on the majority of them while utilizing less memory and processing time.

DenseNet Model

After collecting LBP texture images, they are fed into deep network, which then use the textural images to learn a pattern that best depicts the retinal fundus image of a healthy eye and an eye with glaucoma as shown in Fig. 5. DenseNet-121 is the deep learning model used to complete the binary classification in this work. It has demonstrated effectiveness in previous work in terms of utilizing improved features. Fig. 6 displays the DenseNet-121 architecture, which comprises fore layers of dense blocks with a k = 4 growth rate. The number 121 denotes the total number of network layers in the DensNet-121 network. In reality, this network consists of multiple layers. It is comprised of five convolutions and pooling layers, one classification layer (16), three transition layers (6, 12, 24), and two Dense Blocks (1×1 and 3×3 convolutions). A layer of batch normalization (BN), a rectified linear unit (ReLU) activation, and convolution (convs) are all components of the dense block that is part of the DenseNet-121 architecture. The final dense block is

followed by a global average pooling layer, which is then followed by a Softmax classifier being fed the data. Taking into account the fact that DenseNet-121 contains L layers, the direct connections that correspond to those L layers will be as follows: L (L + 1) 2 [29].

The idea of DenseNet-121 is that it starts with a layer called the convolution layer, followed by the basic pooling layer. After these two layers comes the dense block layer, followed by the progress layer, while the other dense block layer is followed by the change layer, the next dense block layer is followed by the progress layer and finally the characterization layer. In this structure, each dense layer consists of two convolution operations 1×1 convolution that extract features while the rest includes 3×3 convolutions to reduce the depth of the features.

As inputs, each layer takes into consideration the feature maps of all of the layers that came before it, and then each following layer takes into consideration the feature maps of the layer that came after it. The DenseNet-121 promotes the reuse of features and reduces the number of parameters, which increases the ability of the model for detecting glaucoma. Ten epochs were utilized to train the model. In addition, the Cross Entropy loss function has been implemented, along with an Adamax optimizer to improve the weights and a learning rate of 0.01 with a batch size of 16.
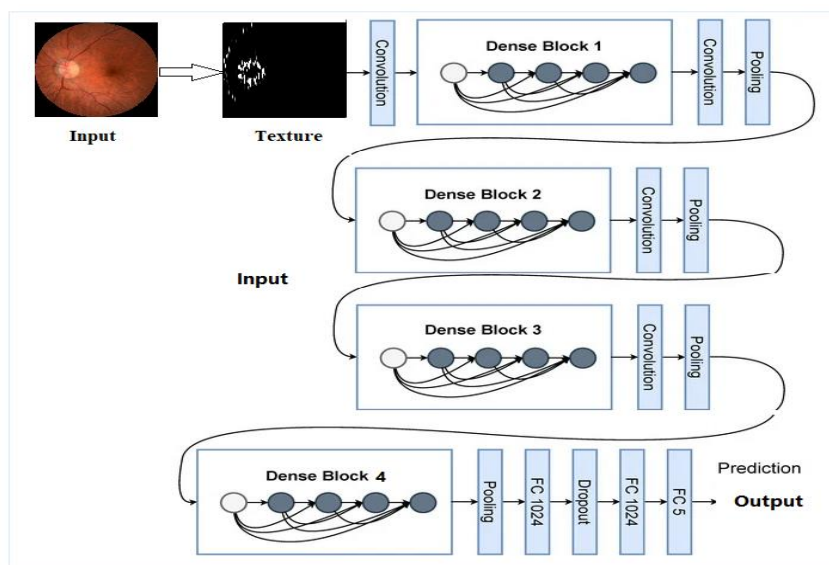
Figure 5. The workflow of the DenseNet-121 architecture used in this study.

Results

The current avatar is required to accurately identify and classify images that have not been previously

detected by the model. The system should possess the capability to accurately differentiate between images exhibiting signs of glaucoma and those belonging to the normal class without any errors. The model is trained to minimize validation loss; hence it is required to accurately identify the correct image class from a given set of input images. Additionally, the model undergoes training with the objective of attaining a high level of accuracy, a process commonly referred to as Model Evaluation. The dataset consists of two distinct classes: one representing normal, healthy retinal eyes, and the other representing retinal eyes affected by glaucoma. For the purpose of evaluation, a total of 130 images were selected from each class to be used for testing. The database has a substantial number of images, from which we have selected 130 images representing the two distinct classes: normal (0) and glaucoma infected (1).
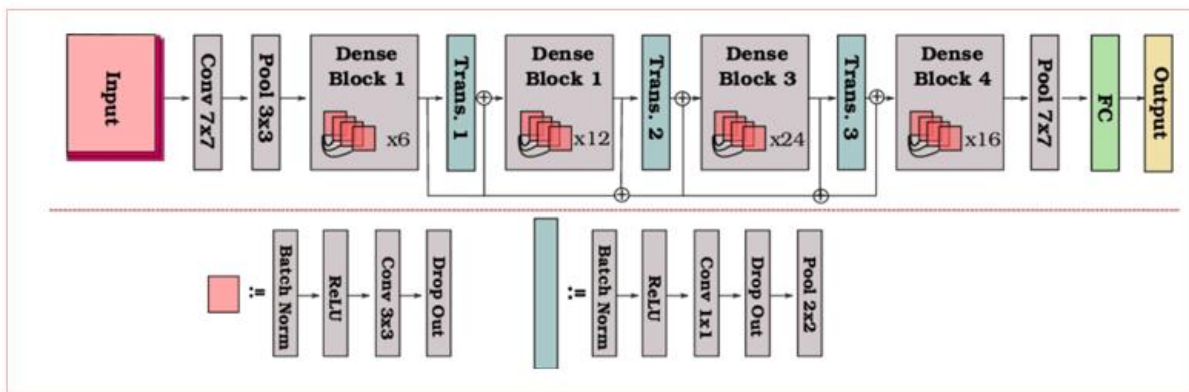
Figure 6. DenseNet-121 architecture [23].

Densenet Optimizers

Within the framework of deep learning, especially CNN, there are many optimizers that can be used to achieve the greatest possible value of accuracy in our proposed model. There are many types of optimizers, including include Stochastic Gradient Descent (often known as SGD), ADAM, AdamW, Adamax, and others. The ADAM optimizer is a combination of the RMSProp algorithm and the SGD algorithm with momentum.

Adam relies on the average of the second moments of the gradients instead of relying on the average of the first moment, which is the basis for the work of the RMSProp algorithm. Despite Adam's effectiveness in performing a separate calculation of the learning rate for each parameter, he still suffers from the problem of weight decay. Another alternative optimizer to Adam, which is an extension of it, is the Adamax optimizer. This optimizer is characterized by its ability to change and adjust the learning rate depending on the characteristics of the input data, so it is suitable for learning data that changes over time, such as texture images that show different contrast for each of the input retinal images. Due to the fact that very few models have embedding's, Adamax is more useful than other optimizers [30]. The concept of Adamax can be understood as a generalization of Adam from the l_2 norm to the l_∞ norm. To define:

$$u_t = B_2^\infty v_{t-1} + (1 - B_2^\infty)|g_t|^\infty \qquad 2$$

Where u_t is the Adamax update rule, B is the beta variable with value 0.999. With the help of the Adamax optimizer and the Cross Entropy loss function, the deep learning-based DenseNet-121 model that was suggested and developed has effectively accomplished an accuracy rate of 96%.

The hyperparameters of the proposed model are shown in Table 1. In fact, these details were relied upon to suit the hardware environment in which the model was trained, where it was used the NVIDIA® GeForce GTX 1050Ti with memory 2GB.

Table 1. Hyperparameters Configurations

Hyperparameters	DenseNet-121
No. of Epoch	10
Batch Size	16
Image Size	224
Learning Step Size	3
Learning Rate	0.01

Accuracy Estimation

This section will discuss the experimental results of the suggested glaucoma detection method. The OIH

dataset's retinal fundus LBP texture images are divided between training and testing at 80–20% with two classes: normal (0) and glaucoma infected (1). Controlling the number of epochs through early stopping using testing accuracy as a monitoring metric. As loss functions, we employed Adam optimizer and binary cross-entropy, with a learning rate of 0.01. In order to assess the accurateness of the proposed system, we employed the metric of accuracy, utilizing commonly used units of measurement. The accuracy is computed using the following formula:

$$Accuracy = \frac{(TP+TN)}{TP+TN+FB+FN} \qquad 3$$

The variables TP, TN, FP, and FN represent true positive, true negative, false positive, and false negative, respectively. Accuracy refers to the comprehensive measure of correctly classified input images. Fig. 7 illustrates the accuracy and loss of the proposed pipeline.

In this part of the analysis, the results of the suggested model were contrasted with the results of earlier research on the OIH. According to Table 2, the performance of the proposed system is much better than that of all other systems when compared to the results of prior studies for all measures.

Table 2. The performance of the proposed model with previous studies

Author	Classification Model	Accuracy
Bhardwaj et al. [31]	Support Vector Machine	92.39 %
Liu et al. [32]	ResNet 50	86.70 %
Junayed et al. [33]	CataractNet	95.02%
Sundaram et al. [34]	hybrid segmentation approach	95.28%
Zhan et al. [35]	Fused CNN models	56.19%
Proposed Model	**DenseNet-121**	**96.35%**
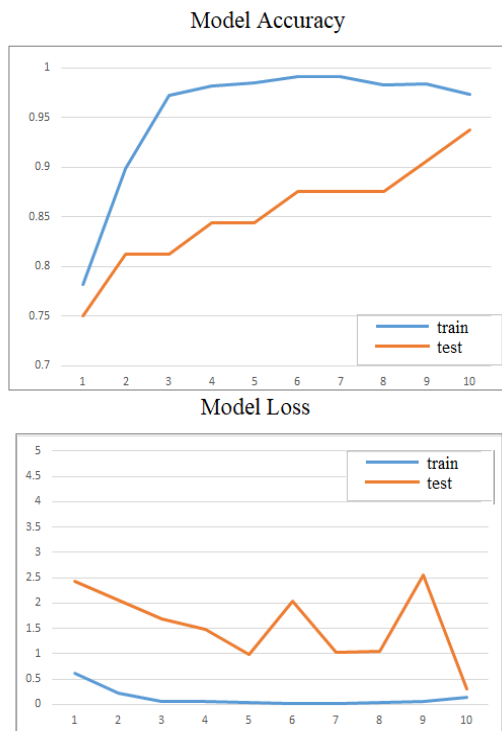
Figure 7. Proposed method accuracy and loss.

Conclusion

This paper proposes a proposed system for identifying glaucoma. The system starts by generating texture images from the entered eye retinal fundus images of the OIH dataset. After this stage, the texture images generated in the previous step are entered into a deep learning model (DenseNet-121) for binary classification. The results indicate that the proposed pipeline has an accuracy rate of 96%.

In the future, we will consider the advantage from the database images in RGB format, as well as the LBP texture images, using a deep learning system that works to extract the properties from the two axes to benefit from all the features in the classification. Furthermore, we intend to carefully assess each network's performance with different hyperparameter settings and tuning.

Authors' Declaration

- Conflicts of Interest: None.
- We hereby confirm that all the Figures and Tables in the manuscript are ours. Furthermore, any Figures and images, that are not ours, have been included with the necessary permission for re-publication, which is attached to the manuscript.

- Ethical Clearance: The project was approved by the local ethical committee at University of Baghdad.
- Ethics statement:
- No animal studies are present in the manuscript.
- No human studies are present in the manuscript.
- No potentially identified images or data are present in the manuscript.

Authors' Contribution Statement

W.J.H, A.S.A. and S.M.S. designed the study, performed the simulations and analyzed the data.

M.J.J. and M.T.I. wrote the paper with input from all authors.

References

1- Ayzenberg V, Kamps FS, Dilks DD, Lourenco SF. Skeletal representations of shape in the human visual cortex. Neuropsychologia. 2022 Jan 7; 164: 108092.https://doi.org/10.1016/j.neuropsychologia.2021.108092

2- Congdon, Nathan, et al. Causes and prevalence of visual impairment among adults in the United States. Arch. Ophth. (Chicago, Ill.: 1960). 2004 Apr 1; 122(4): 477-85.https://doi.org/10.1001/archopht.122.4.477

3- Abdel-Hamid L. Glaucoma detection from retinal images using statistical and textural wavelet features. J Digit Imaging. 2020; 33(1): 151-158. https://doi.org/10.1007/s10278-019-00189-0

4- Kumar BN, Chauhan RP, Dahiya N. Detection of glaucoma using image processing techniques: A critique. Semin Ophthalmol. 2018; 33(2): 275–228.https://doi.org/10.1080/08820538.2016.1229801

5- Kavya N, Padmaja KV. Glaucoma detection using texture features extraction. Proceedings of the 51st IEEE Asilomar Conference on Signals, Systems, and Computers. 2017; 1471–1475.https://doi.org/10.1109/ACSSC.2017.8335600

6- Khalaf M, Dhannoon B N. MSRD-Unet: Multiscale Residual Dilated U-Net for Medical Image Segmentation. Baghdad Sci J. 2022; 19(6 (Suppl.)): 1603-1603.https://doi.org/10.21123/bsj.2022.7559

7- Kadhem S M. Iraqi sign language translator system using deep learning. AJEST. 2023; 2(1): 109-116. https://doi.org/10.55145/ajest.2023.01.01.0013

8- Khalaf M, Dhannoon BN. Skin lesion segmentation based on U-shaped network. Karbala Int J Mod Sci. 2022; 8(3): 493-502. https://doi.org/10.33640/2405-609X.3248

9- Shamsan A, Senan EM, Shatnawi HS. Automatic classification of colour fundus images for prediction eye disease types based on hybrid features. Diagnostics. 2023 May 11; 13(10): 1706. https://doi.org/10.3390/diagnostics13101706

10- Varghese NR, Gopan NR. Performance analysis of automated detection of diabetic retinopathy using machine learning and deep learning techniques. InInnovative Data Communication Technologies and Application: ICIDCA 2019 2020 (pp. 156-164). Springer International Publishing. https://doi.org/10.1007/978-3-030-38040-3_18

11- Iyyanarappan A, Tamilpavai G. Glaucomatous image classification using wavelet-based energy features and PNN. IJTEEE. 2014; 2(4). https://doi.org/10.1109/TITB.2011.2176540

12- Biswal B, Vyshnavi E, Sairam MV. Robust retinal optic disc and optic cup segmentation via stationary wavelet transform and maximum vessel pixel sum. IET Image Process. 14 (4): 592–602. https://doi.org/10.1049/iet-ipr.2019.0845

13- Singh A, Dutta MK, ParthaSarathi M, Uher V, Burget R. Image processing based automatic diagnosis of glaucoma using wavelet features of segmented optic disc from fundus image. Comput. Methods Programs Biomed. 2016 Feb 1; 124: 108-20. https://doi.org/10.1016/j.cmpb.2015.10.010

14- Dutta MK, Mourya AK, Singh A, Parthasarathi M, Burget R, Riha K. Glaucoma detection by segmenting the super pixels from fundus colour retinal images. In2014 international conference on medical imaging, m-health and emerging communication systems (MedCom) 2014 Nov 7 (pp. 86-90). IEEE. https://doi.org/10.1109/MedCom.2014.7005981

15- Dey N, Roy AB, Das A, Chaudhuri SS. Optical cup to disc ratio measurement for glaucoma diagnosis using harris corner. In2012 Third International Conference on Computing, Communication and Networking Technologies (ICCCNT'12) 2012 Jul 26 (pp. 1-5). IEEE. https://doi.org/10.1109/ICCCNT.2012.6395971 .

16- Guru Prasad MS, Naveen Kumar HN, Raju K, Santhosh Kumar DK, Chandrappa S. Glaucoma detection using clustering and segmentation of the optic disc region from retinal fundus images. SN Comput. Sci. 2023 Feb 2; 4(2): 192. https://doi.org/10.1007/s42979-022-01592-1

17- Nawaldgi S, Lalitha YS. Automated glaucoma assessment from color fundus images using structural and texture features. Biomed Signal Process. Control. 2022 Aug 1; 77:103875. https://doi.org/10.1016/j.bspc.2022.103875

18- Bechar ME, Settouti N, Barra V, Chikh MA. Semi-supervised superpixel classification for medical images segmentation: application to detection of glaucoma disease. Multidimension Syst Signal Process. 2018 Jul; 29: 979-98. https://doi.org/10.1007/s11045-017-0483-y

19- Thakur N, Juneja M. Survey on segmentation and classification approaches of optic cup and optic disc for diagnosis of glaucoma. Biomed Signal Process Control. 2018 Apr 1; 42: 162-89. https://doi.org/10.1016/j.bspc.2018.01.014

20- Spaeth GL, Lopes JF, Junk AK, Grigorian AP, Henderer J. Systems for staging the amount of optic nerve damage in glaucoma: a critical review and new material. Surv Ophthalmol. 2006 Jul 1; 51(4): 293-315. https://doi.org/10.1016/j.survophthal.2006.04.008

21- Khalil T, Usman Akram M, Khalid S, Jameel A. Improved automated detection of glaucoma from fundus image using hybrid structural and textural features. IET Image Proc. 2017 Sep; 11(9): 693-700. https://doi.org/10.1049/iet-ipr.2016.0812

22- Barros DM, Moura JC, Freire CR, Taleb AC, Valentim RA, Morais PS. Machine learning applied to retinal image processing for glaucoma detection: review and perspective. Biomed Eng Online. 2020 Dec; 19: 1-21. https://doi.org/10.1186/s12938-020-00767-2

23- Ojala T, Pietikainen M, Maenpaa T. Multiresolution gray-scale and rotation invariant texture classification with local binary patterns. IEEE Trans Pattern Anal Mach Intell. 2002 Jul; 24(7): 971-87. https://doi.org/10.1109/TPAMI.2002.1017623

24- Vu HN, Nguyen MH, Pham C. Masked face recognition with convolutional neural networks and local binary patterns. Appl Intell. 2022 Mar; 52(5): 5497-512. https://doi.org/10.1007/s10489-021-02728-1

25- Chauhan T, Palivela H, Tiwari S. Optimization and fine-tuning of DenseNet model for classification of COVID-19 cases in medical imaging. InInt JInf Manage Data Insights. 2021 Nov 1; 1(2): 100020. https://doi.org/10.1016/j.jjimei.2021.100020

26- Zhang C, Benz P, Argaw DM, Lee S, Kim J, Rameau F, Bazin JC, Kweon IS. Resnet or densenet? introducing dense shortcuts to resnet. InProceedings of the IEEE/CVF winter conference on applications of computer vision 2021 (pp. 3550-3559).https://doi.org/10.1109/WACV48630.2021.00359

27- Huang G, Chen D, Li T, Wu F, Van Der Maaten L, Weinberger KQ. Multi-scale dense networks for resource efficient image classification. arXiv preprint arXiv:1703.09844. 2017 Mar 29. 2017; 1703: 09844. https://doi.org/10.48550/arXiv.1703.09844

28- Huang G, Liu Z, Van Der Maaten L, Weinberger KQ. Densely connected convolutional networks. InProceedings of the IEEE conference on computer vision and pattern recognition 2017 (pp. 4700-4708). https://doi.org/10.1109/CVPR.2017.243

29- Sreena VG, Ponraj DN. Optimization of Fine Tuned Deep Learning Model for Multiclass Classification of Chest X-Rays. In2023 4th International Conference on Signal Processing and Communication (ICSPC) 2023 Mar 23 (pp. 173-177). IEEE. https://doi.org/10.1109/ICSPC57692.2023.10126060

30- Kingma DP, Ba J. Adam: A method for stochastic optimization. arXiv preprint arXiv:1412.6980. 2014 Dec 22. https://doi.org/10.48550/arXiv.1412.6980

31- Bhardwaj C, Jain S, Sood M. Hierarchical severity grade classification of non-proliferative diabetic retinopathy. J Ambient Intell. Hum Comput.. 2021 Feb; 12(2): 2649-70. https://doi.org/10.1007/s12652-020-02426-9

32- Liu S, Graham SL, Schulz A, Kalloniatis M, Zangerl B, Cai W, et al. A deep learning-based algorithm identifies glaucomatous discs using monoscopic fundus photographs. Ophthalmol Glaucoma. 2018; 1(1) : 15-22. https://doi.org/10.3390/healthcare10122345

33- Junayed MS, Islam MB, Sadeghzadeh A, Rahman S. CataractNet: An automated cataract detection system using deep learning for fundus images. IEEE access. 2021 Sep 15; 9: 128799-808. https://doi.org/10.1109/ACCESS.2021.3112938

34- Sundaram R, Ks R, Jayaraman P. Extraction of blood vessels in fundus images of retina through hybrid segmentation approach. Mathematics. 2019 Feb 13; 7(2): 169. https://doi.org/10.3390/math7020169

35- Olayah F, Senan EM, Ahmed IA, Awaji B. AI techniques of dermoscopy image analysis for the early detection of skin lesions based on combined CNN features. Diagnostics. 2023 Apr 1; 13(7): 1314. https://doi.org/10.3390/diagnostics13071314

نموذج الشبكة الكثيفة لتقييم أداء تصنيف الجلوكوما الثنائي مع استخدام ميزة الملمس

ولدان جميل هادي، امال سفيح عجرش، سحر منعم سلمان، ميس جلال جاسم، مينا طه إبراهيم

قسم علوم الحاسوب، كلية العلوم للبنات، جامعة بغداد، بغداد، العراق.

الخلاصة

تعتبر شبكية العين جزءًا مهمًا من العين لأن الأطباء يستخدمون صورها لتشخيص العديد من أمراض العيون مثل الجلوكوما واعتلال الشبكية السكري وإعتام عدسة العين. في الواقع، يعد تصوير الشبكية المجزأ أداة قوية للكشف عن النمو غير العادي في منطقة العين بالإضافة إلى تحديد حجم وبنية القرص البصري. يمكن أن يؤدي الجلوكوما إلى إتلاف القرص البصري، مما يغير مظهر القرص البصري للعين. تعمل تقنيتنا على الكشف عن الجلوكوما وتصنيفها في هذه الدراسة. تستخدم المرحلة الأولى من هذا النظام الأنماط الثنائية المحلية (LBPللحصول على خرائط للميزات التركيبية. يتم تنفيذ التصنيف الثنائي لصور الجلوكوما بشكل منفصل عن الصور العادية باستخدام تقنية التعلم العميق في الخطوة الثانية من هذا النظام. بالنسبة لتحديات التصنيف، استخدمنا تقنية الشبكة الكثيفة، وهي تقنية التعلم العميق. وتبقى دقتها في حدود 96% حسب نتائج الطريقة المقترحة.

الكلمات المفتاحية: التصنيف الثنائي، DenseNet، أمراض العيون، LBP، الملمس.